

RCS2D: A 2D MoM and FDTD-Based Scattering Simulator

Gizem Toroğlu,¹ Mehmet Alper Uslu,¹ Levent Sevgi^{1,2}

¹ Electronics and Communications Engineering Department, Doğuş University, 34722 Istanbul, Turkey

² Electrical and Computer Engineering Department, University of Massachusetts, Lowell, MA

Received 18 July 2012; accepted 26 December 2012

ABSTRACT: A Java-based, two-dimensional electromagnetic (EM) scattering field simulator—RCS2D—is introduced. It enables one to explore EM wave—arbitrary object interaction under a plane wave illumination. RCS2D uses both method of moments and finite-difference time-domain models for both transverse magnetic and transverse electric polarizations. © 2013 Wiley Periodicals, Inc. *Int J RF and Microwave CAE* 23:437–443, 2013.

Keywords: electromagnetic waves; scattering; radar cross section (RCS); MoM; FDTD; transverse magnetic; transverse electric

I. INTRODUCTION

Electromagnetic (EM) scattering concerns interaction of waves with objects and has many applications in modern radar systems, low-visible target design, cancer detection, mine exploration, and so forth. Scattering problems can be classified as inverse and direct scattering. Inverse scattering aims to determine the object (scatterer) from the knowledge of asymptotic behavior of scattered fields (SFs). Direct scattering aims to find out SFs from known incident field and the object. The former depends extensively on the latter. A Java-based, two-dimensional (2D) EM scattering simulator—RCS2D—is introduced to explore scattering behavior of variety of materials with different geometries and material properties. The 2D scenario used in RCS2D is shown in Figure 1. An infinitely long cylinder with arbitrary cross-section illuminated by a plane wave (PW) from a specified direction is taken into account. Two types of solutions are of interest: transverse magnetic (TM) and transverse electric (TE).

RCS2D performs simulations with both Method of Moments (MoM) and Finite-Difference Time-Domain (FDTD) models. The user may create an arbitrary shaped, dielectric and/or diamagnetic objects and do the scattering analysis for both TM and TE polarizations.

II. THE METHOD OF MOMENT MODEL

MoM is a frequency domain model and has been in use since 1960s [1]. It is based on the discretization/reduction

of time-harmonic EM field integral equations into a linear matrix system. MoM model for dielectric cylinders of arbitrary cross section was first proposed by Richmond in Ref. 2 and then generalized to dielectric/diamagnetic objects with oblique incident case in Ref. 3. For the sake of completeness, we summarize necessary equations to find scattering fields for both for TM_z and TE_z polarizations [3].

A. TM_z Polarization Case

The incident PW for the TM_z case is in the form of:

$$E_z^{(inc)} = E_0 e^{jk_0(x(n)\cos(\phi) + y(n)\sin(\phi))} \quad (1)$$

$$H_x^{(inc)} = \frac{E_0 k_0 \sin(\phi)}{\mu\omega} E_z^{(inc)}; H_y^{(inc)} = -\frac{E_0 k_0 \cos(\phi)}{\mu\omega} E_z^{(inc)} \quad (2)$$

where ϕ is the incident angle, k_0 is the free space wave number, E_0 is the amplitude of the incident electric field and N is the total number of cells ($n = 1, 2, \dots, N$).

After calculating incident fields, $3N \times 1$ Y matrix is constructed as:

$$Y = [E_z^{(inc)} \quad \eta_0 H_x^{(inc)} \quad \eta_0 H_y^{(inc)}]^T \quad (3)$$

where η_0 is the free space wave impedance.

The incident fields create surface currents on the surface of the object and that currents produce SFs. As total field (TF) is the summation of incident and SFs we can write:

$$E_z = E_z^{inc} + E_z^s; H_x = H_x^{inc} + H_x^s; H_y = H_y^{inc} + H_y^s \quad (4)$$

Correspondence to: G. Toroğlu; e-mail: torogluzim@yahoo.com)

DOI 10.1002/mmce.20731

Published online 2 May 2013 in Wiley Online Library (wileyonlinelibrary.com).

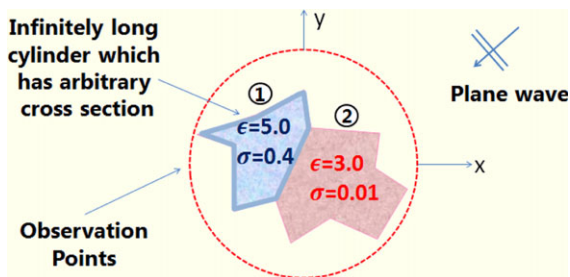


Figure 1 Cross section of an object under investigation and a PW illumination from a given direction. [Color figure can be viewed in the online issue, which is available at wileyonlinelibrary.com]

In MoM, the cross section of the object under investigation is divided into small pieces (compared to wavelength). The problem is discretized accordingly and matrix form is acquired:

$$[Z] [E_z \ \eta_0 H_x \ \eta_0 H_y]^T = Y. \quad (5)$$

The $3N \times 3N$ Z matrix is then expressed as:

$$Z = \begin{bmatrix} A & B & C \\ D & E & F \\ G & F & H \end{bmatrix} \quad (6)$$

where the entries of the Z matrix are ($m, n = 1, 2, \dots, N$):

$$A_{mn} = \begin{cases} -(\epsilon_{rn} - 1) \frac{\pi k a_n}{2j} J_1(k a_n) H_0^{(2)}(k \rho_{mn}) & m \neq n \\ 1 + \frac{j}{2} (\epsilon_{rn} - 1) [\pi k a_n H_1^{(2)}(k a_n) - 2j] & m = n \end{cases} \quad (7)$$

$$B_{mn} = \begin{cases} \frac{\pi k a_n}{2} J_1(k a_n) (\mu_{rn} - 1) (y_m - y_n) \frac{H_1^{(2)}(k \rho_{mn})}{\rho_{mn}} & m \neq n \\ 0 & m = n \end{cases} \quad (8)$$

$$C_{mn} = \begin{cases} -\frac{\pi k a_n}{2} J_1(k a_n) (\mu_{rn} - 1) (x_m - x_n) \frac{H_1^{(2)}(k \rho_{mn})}{\rho_{mn}} & m \neq n \\ 0 & m = n \end{cases} \quad (9)$$

$$D_{mn} = \begin{cases} \frac{\pi k a_n}{2} J_1(k a_n) (\epsilon_{rn} - 1) (y_m - y_n) \frac{H_1^{(2)}(k \rho_{mn})}{\rho_{mn}} & m \neq n \\ 0 & m = n \end{cases} \quad (10)$$

$$E_{mn} = \begin{cases} 1 + \frac{j(\mu_{rn}-1)}{4} [\pi k a_n H_1^{(2)}(k a_n) - 4j] & m = n \\ \frac{(\mu_{rn}-1)\pi j k a_n}{2} J_1(K a_n) \frac{-1}{(k \rho_{mn})^3} & \\ -k^3 \rho_{mn} (y_m - y_n)^2 H_0^{(2)}(k \rho_{mn}) & \\ + [(y_m - y_n)^2 - (x_m - x_n)^2] k^2 H_1^{(2)}(k \rho_{mn}) & m \neq n \end{cases} \quad (11)$$

$$F_{mn} = \begin{cases} 0 & m = n \\ -\frac{(\mu_{rn}-1)\pi k a_n J_1(k a_n) k^2}{2j(k \rho_{mn})^3} (x_m - x_n) (y_m - y_n) & \\ (2H_1^{(2)}(k \rho_{mn}) - k \rho_{mn} H_0^{(2)}(k \rho_{mn})) & m \neq n \end{cases} \quad (12)$$

$$G_{mn} = \begin{cases} \frac{-\pi k a_n}{2} J_1(k a_n) (\epsilon_{rn} - 1) (x_m - x_n) \frac{H_1^{(2)}(k \rho_{mn})}{\rho_{mn}} & m \neq n \\ 0 & m = n \end{cases} \quad (13)$$

$$H_{mn} = \begin{cases} 1 + \frac{j(\mu_{rn}-1)}{4} [\pi k a_n H_1^{(2)}(k a_n) - 4j] & m = n \\ \frac{(\mu_{rn}-1)\pi j k a_n}{2} J_1(K a_n) \frac{1}{(k \rho_{mn})^3} & \\ -k^3 \rho_{mn} (x_m - x_n)^2 H_0^{(2)}(k \rho_{mn}) & \\ + [(x_m - x_n)^2 - (y_m - y_n)^2] k^2 H_1^{(2)}(k \rho_{mn}) & m \neq n \end{cases} \quad (14)$$

where $a_{m,n}$ is the area of rectangular cell at the location of m or n , $\mu_{r\{n,m\}}$ is the relative magnetic permeability of the n th or m th cell and $\epsilon_{r\{n,m\}}$ is the relative electric permittivity of the n th or m th cell.

After Z matrix is formed, electric field can be calculated by means of (5):

$$\begin{bmatrix} E_z \\ \eta_0 H_x \\ \eta_0 H_y \end{bmatrix} = [Z]^{-1} \begin{bmatrix} E_z^{(inc)} \\ \eta_0 H_x^{(inc)} \\ \eta_0 H_y^{(inc)} \end{bmatrix} \quad (15)$$

The electric field component of the SF at any point outside the dielectric body can be found by:

$$E_z^s = j \frac{\pi}{2} \sqrt{\frac{2j}{\pi}} \sum_{n=1}^N k a_n J_1(k a_n) \frac{[(\mu_{rn} - 1) [\eta_0 H_{yn} \cos \phi - \eta_0 H_{xn} \sin \phi] - (\epsilon_{rn} - 1) E_{zn}]}{\sqrt{k \rho_0} e^{jk(x_n \cos \phi + y_n \sin \phi)} e^{-jk r_0}} \quad (16)$$

SFs can also be represented in terms of the Radar Cross Section (RCS, σ) as:

$$\sigma(\phi) = \lim_{\rho_0 \rightarrow \infty} 2\pi \rho_0 \left| \frac{E_z^s(\rho_0, \phi)}{E_z^{(inc)}} \right|^2 \quad (17)$$

where ϕ is the observation angle.

B. TE_z Polarization Case

The incident field components for this polarization can be calculated from:

$$H_z^{(inc)} = H_0 e^{jk_0(x(n) \cos(\phi) + y(n) \sin(\phi))} \quad (19)$$

$$E_x^{(inc)} = -\frac{E_0 k_0 \text{Sin}(\phi)}{\epsilon \omega} H_z^{(inc)} \quad (20)$$

$$E_y^{(inc)} = \frac{E_0 k_0 \text{Cos}(\phi)}{\epsilon \omega} H_z^{(inc)} \quad (21)$$

Corresponding field vectors are constructed as:

$$Y = \begin{bmatrix} E_x^{(inc)} \\ E_y^{(inc)} \\ \eta_0 H_z^{(inc)} \end{bmatrix}; [Z] \begin{bmatrix} E_x \\ E_y \\ \eta_0 H_z \end{bmatrix} = \begin{bmatrix} E_x^{(inc)} \\ E_y^{(inc)} \\ \eta_0 H_z^{(inc)} \end{bmatrix} \quad (22)$$

Construction of Z matrix is similar to TM_z mode where

$$A_{mn} = \begin{cases} 1 + \frac{j(\epsilon_{rn}-1)}{4} [\pi k a_m H_1^{(2)}(k a_m) - 4j] & m = n \\ \frac{(\epsilon_{rn}-1)\pi j k a_n}{2} J_1(K a_n) \frac{-1}{(k \rho_{mn})^3} & m \neq n \\ \begin{bmatrix} -k^3 \rho_{mn} (y_m - y_n)^2 H_0^{(2)}(k \rho_{mn}) \\ + [(y_m - y_n)^2 - (x_m - x_n)^2] k^2 H_1^{(2)}(k \rho_{mn}) \end{bmatrix} & m \neq n \end{cases} \quad (23)$$

$$B_{mn} = \begin{cases} -\frac{(\epsilon_{rn}-1)\pi K a_n J_1(K a_n)}{2j(K \rho_{mn})^3} K^2 (x_m - x_n)(y_m - y_n) & m \neq n \\ [2H_1^{(2)}(K \rho_{mn}) - K \rho_{mn} H_0^{(2)}(K \rho_{mn})] & m = n \\ 0 & m = n \end{cases} \quad (24)$$

$$C_{mn} = \begin{cases} -\frac{\pi k a_n}{2} J_1(k a_n) (\mu_{rn} - 1) (y_m - y_n) \frac{H_1^{(2)}(k \rho_{mn})}{\rho_{mn}} & m \neq n \\ 0 & m = n \end{cases} \quad (25)$$

$$D_{mn} = \begin{cases} \frac{(\epsilon_{rn}-1)\pi j k a_n}{2} J_1(K a_n) \frac{1}{(k \rho_{mn})^3} & m \neq n \\ \begin{bmatrix} -k^3 \rho_{mn} (x_m - x_n)^2 H_0^{(2)}(k \rho_{mn}) \\ + [(x_m - x_n)^2 - (y_m - y_n)^2] k^2 H_1^{(2)}(k \rho_{mn}) \end{bmatrix} & m \neq n \\ 1 + \frac{j(\epsilon_{rn}-1)}{4} [\pi k a_m H_1^{(2)}(k a_m) - 4j] & m = n \end{cases} \quad (26)$$

$$E_{mn} = \begin{cases} \frac{\pi k a_n}{2} J_1(k a_n) (\mu_{rn} - 1) (x_m - x_n) \frac{H_1^{(2)}(k \rho_{mn})}{\rho_{mn}} & m \neq n \\ 0 & m = n \end{cases} \quad (27)$$

$$F_{mn} = \begin{cases} -\frac{\pi k a_n}{2} J_1(k a_n) (\epsilon_{rn} - 1) (y_m - y_n) \frac{H_1^{(2)}(k \rho_{mn})}{\rho_{mn}} & m \neq n \\ 0 & m = n \end{cases} \quad (28)$$

$$G_{mn} = \begin{cases} \frac{\pi k a_n}{2} J_1(k a_n) (\epsilon_{rn} - 1) (x_m - x_n) \frac{H_1^{(2)}(k \rho_{mn})}{\rho_{mn}} & m \neq n \\ 0 & m = n \end{cases} \quad (29)$$

$$H_{mn} = \begin{cases} -(\mu_{rn} - 1) \frac{\pi k a_n}{2j} J_1(k a_n) H_0^{(2)}(k \rho_{mn}) & m \neq n \\ 1 + \frac{j}{2} (\mu_{rn} - 1) [\pi k a_m H_1^{(2)}(k a_m) - 2j] & m = n \end{cases} \quad (30)$$

Scattered magnetic field for this mode can be found by:

$$H_z^s = j \frac{\pi}{2} \sqrt{\frac{2j}{\pi}} \sum_{n=1}^N k a_n J_1(k a_n) \times [(\epsilon_{rn} - 1) [-E_{yn} \cos \phi + E_{xn} \sin \phi] - (\mu_{rn} - 1) \eta_0 H_{zn}] \times e^{jk(x_n \cos \phi + y_n \sin \phi)} \frac{e^{-jk r_0}}{\sqrt{k \rho_0}} \quad (31)$$

III. THE FDTD MODEL

The Finite Difference Time Domain (FDTD) model was first proposed by Yee in 1966 [4]. It is based on the application of second-order centered differences to time and spatial derivatives of Maxwell equations. FDTD is a time domain based method, but it is easy to obtain frequency domain responses via Fourier Transform. Because of its fi-

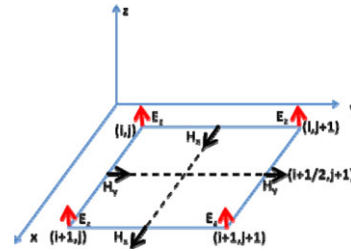


Figure 2 Yee Cell for TM_z polarization in 2D. [Color figure can be viewed in the online issue, which is available at wileyonlinelibrary.com]

nite nature, original Yee algorithm should be modified at the terminals of the simulation space, and in addition, a kind of near-to-far field (NTFF) transformation is required to handle RCS problems. There are several terminations proposed so far but the most powerful one in terms of absorption characteristics is the perfectly matched layer (PML) termination [5]. Among PML types, CPML [6] is used in RCS2D because of its superior absorbing performance.

A. TM_z Polarization Case

The 2D YEE cell is pictured in Figure 2. In addition to spatial offset between electric and magnetic fields there is also half time step offset. Once spatial and time arrangements of field components are known, Faraday and Ampere laws can be discretized by the application of second-order central differences. The choice of spatial steps Δx and Δy affects anisotropy of the numerical phase velocity, besides they can roughly be chosen as $\Delta x, \Delta y \leq \lambda/10$. The time step Δt is related to stability [7].

$$\Delta t < 1 \sqrt{((1/\Delta x)^2 + (1/\Delta y)^2)}$$

1. TF/SF Formulation. Short dipoles (excitation) can be included via either soft or hard injections and is straightforward. However, PW injection is a little bit complicated. One of the most widely used methods for this purpose is TF/SF formulation [7]. Here, the simulation area is divided into two regions: TF region (inside) where incident PW and scattering object appear, and SF region (outside) where only SFs exist (Fig. 3).

EM field components for this formulation are as shown in Figure 4.

Iterative equations for the critical nodes are:

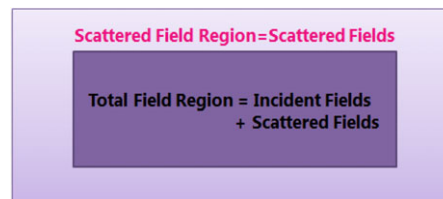


Figure 3 TF/SF representation. [Color figure can be viewed in the online issue, which is available at wileyonlinelibrary.com]

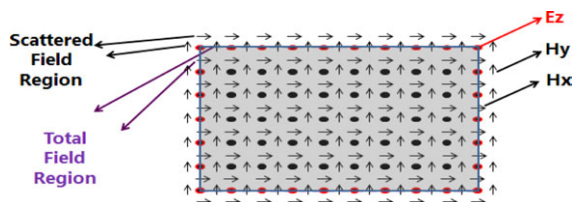


Figure 4 TF/SF representation of TM_z mode. [Color figure can be viewed in the online issue, which is available at wileyonlinelibrary.com]

Inside—Front Face ($j = j_0; i = i_0, \dots, i_1$):

$$E_z|_{i,j_0}^{n+1} = \{E_z|_{i,j_0}^{n+1}\} + \frac{\Delta t}{\epsilon_0 \Delta} H_{x,inc}|_{i,j_0-1/2}^{n+1/2} \quad (32)$$

Inside—Back Face ($j = j_1; i = i_0, \dots, i_1$):

$$E_z|_{i,j_1}^{n+1} = \{E_z|_{i,j_1}^{n+1}\} - \frac{\Delta t}{\epsilon_0 \Delta} H_{x,inc}|_{i,j_1+1/2}^{n+1/2} \quad (33)$$

Inside—Left Face ($i = i_0; j = j_0, \dots, j_1$):

$$E_z|_{i_0,j}^{n+1} = \{E_z|_{i_0,j}^{n+1}\} - \frac{\Delta t}{\epsilon_0 \Delta} H_{y,inc}|_{i_0-1/2,j}^{n+1/2} \quad (34)$$

Inside—Right Face ($i = i_1; j = j_0, \dots, j_1$):

$$E_z|_{i_1,j}^{n+1} = \{E_z|_{i_1,j}^{n+1}\} + \frac{\Delta t}{\epsilon_0 \Delta} H_{y,inc}|_{i_1+1/2,j}^{n+1/2} \quad (35)$$

Inside—Outside Front Face ($j = j_0 - 1/2; i = i_0, \dots, i_1$):

$$H_x|_{i,j_0-1/2}^{n+1/2} = \{H_x|_{i,j_0-1/2}^{n+1/2}\} + \frac{\Delta t}{\mu_0 \Delta} E_{z,inc}|_{i,j_0}^n \quad (36)$$

Inside—Outside Back Face ($j = j_1 + 1/2; i = i_0, \dots, i_1$):

$$H_x|_{i,j_1+1/2}^{n+1/2} = \{H_x|_{i,j_1+1/2}^{n+1/2}\} - \frac{\Delta t}{\mu_0 \Delta} E_{z,inc}|_{i,j_1}^n \quad (37)$$

Inside—Outside Back Face ($i = i_0 - 1/2; j = j_0, \dots, j_1$):

$$H_y|_{i_0-1/2,j}^{n+1/2} = \{H_y|_{i_0-1/2,j}^{n+1/2}\} - \frac{\Delta t}{\mu_0 \Delta} E_{z,inc}|_{i_0,j}^n \quad (38)$$

Inside—Outside Right Face ($i = i_1 + 1/2; j = j_0, \dots, j_1$):

$$H_y|_{i_1+1/2,j}^{n+1/2} = \{H_y|_{i_1+1/2,j}^{n+1/2}\} - \frac{\Delta t}{\mu_0 \Delta} E_{z,inc}|_{i_1,j}^n \quad (39)$$

The incident field is propagated by applying appropriate delay at necessary field locations:

$$n_{delay} = \frac{d \Delta}{v_p(\phi) \Delta t} \quad (40)$$

where v_p is the numerical phase velocity of the incident wave at the propagation angle ϕ . Here, distance d can be calculated from:

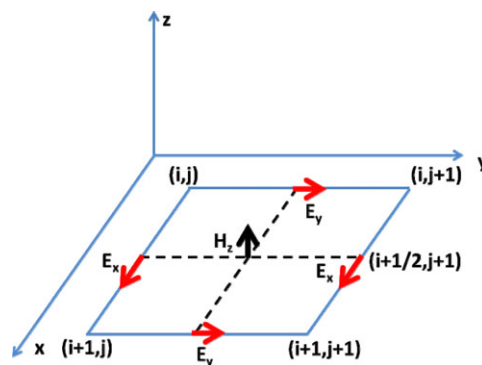


Figure 5 Yee Cell for TE_z polarization in 2D. [Color figure can be viewed in the online issue, which is available at wileyonlinelibrary.com]

$$d = \tilde{k}_{inc} \cdot \vec{r}_{comp} \quad \text{where} \quad (41)$$

$$\tilde{k}_{inc} = \hat{x} \cos(\phi) + \hat{y} \sin(\phi) \quad \text{and}$$

$$\vec{r}_{comp} = (i_{comp} - i_0) \hat{x} + (j_{comp} - j_0) \hat{y}$$

i_{comp} and j_{comp} can be either integers or integers $\pm 1/2$. Also, i_0 and j_0 are the first TF cell contacted by the incident PW. For the sake of completeness, we presented whole origin points and corresponding r_{comp} vectors as shown below:

$0^\circ \leq \phi < 90^\circ$	Origin(i_0, j_0)	(42)
$90^\circ \leq \phi < 180^\circ$	Origin(i_1, j_0)	
$180^\circ \leq \phi < 270^\circ$	Origin(i_1, j_1)	
$270^\circ \leq \phi < 360^\circ$	Origin(i_0, j_1)	

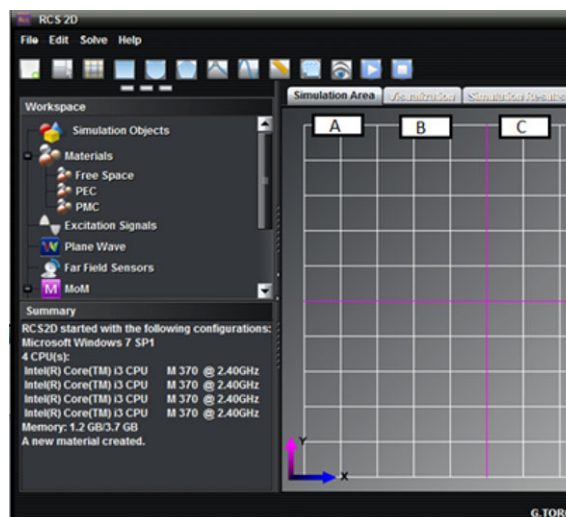


Figure 6 The part of user interface of RCS2D Virtual Tool (A: the simulation area, B: visualizations, C: simulation results). [Color figure can be viewed in the online issue, which is available at wileyonlinelibrary.com]

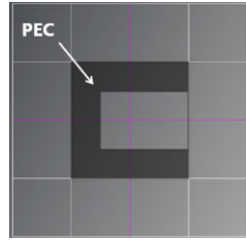


Figure 7 The C-shaped PEC object. [Color figure can be viewed in the online issue, which is available at wileyonlinelibrary.com]

$$\begin{aligned}
 0^\circ \leq \phi < 90^\circ & \quad \hat{\Gamma}_{\text{comp}} = (i_{\text{comp}} - i_0)\hat{x} + (j_{\text{comp}} - j_0)\hat{y} \\
 90^\circ \leq \phi < 180^\circ & \quad \hat{\Gamma}_{\text{comp}} = (i_{\text{comp}} - i_1)\hat{x} + (j_{\text{comp}} - j_0)\hat{y} \\
 180^\circ \leq \phi < 270^\circ & \quad \hat{\Gamma}_{\text{comp}} = (i_{\text{comp}} - i_1)\hat{x} + (j_{\text{comp}} - j_1)\hat{y} \\
 270^\circ \leq \phi < 360^\circ & \quad \hat{\Gamma}_{\text{comp}} = (i_{\text{comp}} - i_0)\hat{x} + (j_{\text{comp}} - j_1)\hat{y}
 \end{aligned} \tag{43}$$

B. TE_z Polarization Case

The Yee cell in this case is given in Figure 5.

1. TF/SF Formulation. Iterative equations for the critical nodes are:

Inside—Front Face ($j = j_0; i = i_0, \dots, i_1 - 1$):

$$E_x|_{i,j_0}^{n+1} = \{E_x|_{i,j_0}^{n+1}\} + \frac{\Delta t}{\epsilon_0 \Delta} H_{z,\text{inc}}|_{i,j_0-1/2}^{n+1/2} \tag{44}$$

Inside—Back Face ($j = j_1; i = i_0, \dots, i_1 - 1$):

$$E_x|_{i,j_1}^{n+1} = \{E_x|_{i,j_1}^{n+1}\} - \frac{\Delta t}{\epsilon_0 \Delta} H_{z,\text{inc}}|_{i,j_1+1/2}^{n+1/2} \tag{45}$$

Inside—Left Face ($i = i_0; j = j_0, \dots, j_1 - 1$):

$$E_y|_{i_0,j}^{n+1} = \{E_y|_{i_0,j}^{n+1}\} - \frac{\Delta t}{\epsilon_0 \Delta} H_{z,\text{inc}}|_{i_0-1/2,j}^{n+1/2} \tag{46}$$

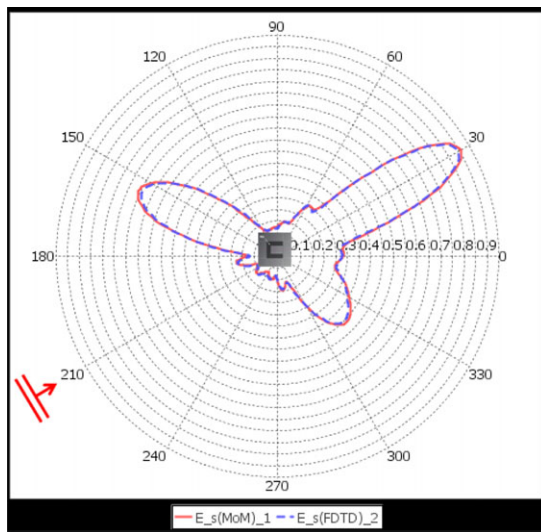


Figure 8 The SF of C-shaped PEC object (TM_z mode, $f = 600$ MHz, illumination angle = 210°). [Color figure can be viewed in the online issue, which is available at wileyonlinelibrary.com]

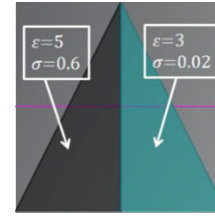


Figure 9 The second test cylinder. [Color figure can be viewed in the online issue, which is available at wileyonlinelibrary.com]

Inside—Right Face ($i = i_1; j = j_0, \dots, j_1 - 1$):

$$E_y|_{i_1,j}^{n+1} = \{E_y|_{i_1,j}^{n+1}\} + \frac{\Delta t}{\epsilon_0 \Delta} H_{z,\text{inc}}|_{i_1+1/2,j}^{n+1/2} \tag{47}$$

Inside—Outside Front Face ($j = j_0 - 1/2; i = i_0, \dots, i_1$):

$$H_z|_{i,j_0-1/2}^{n+1/2} = \{H_z|_{i,j_0-1/2}^{n+1/2}\} + \frac{\Delta t}{\mu_0 \Delta} E_{x,\text{inc}}|_{i,j_0}^n \tag{48}$$

Inside—Outside Back Face ($j = j_1 + 1/2; i = i_0, \dots, i_1$):

$$H_z|_{i,j_1+1/2}^{n+1/2} = \{H_z|_{i,j_1+1/2}^{n+1/2}\} - \frac{\Delta t}{\mu_0 \Delta} E_{x,\text{inc}}|_{i,j_1}^n \tag{49}$$

Inside—Outside Left Face ($i = i_0 - 1/2; j = j_0, \dots, j_1$):

$$H_z|_{i_0-1/2,j}^{n+1/2} = \{H_z|_{i_0-1/2,j}^{n+1/2}\} - \frac{\Delta t}{\mu_0 \Delta} E_{y,\text{inc}}|_{i_0,j}^n \tag{50}$$

Inside—Outside Right Face ($i = i_1 + 1/2; j = j_0, \dots, j_1$):

$$H_z|_{i_1+1/2,j}^{n+1/2} = \{H_z|_{i_1+1/2,j}^{n+1/2}\} - \frac{\Delta t}{\mu_0 \Delta} E_{y,\text{inc}}|_{i_1,j}^n \tag{51}$$

The rest of the calculations concerning TF/SF formulation are similar to TM_z polarization case.

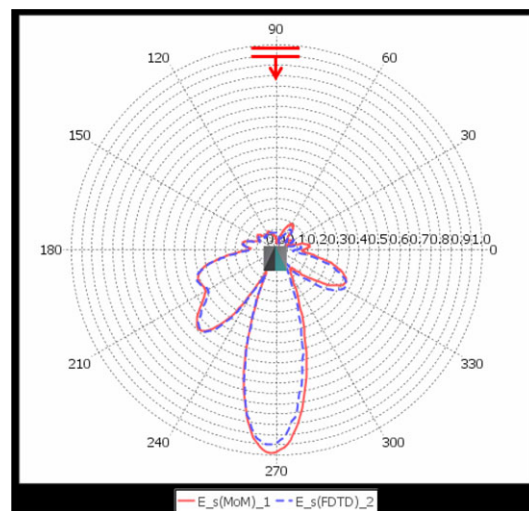


Figure 10 The SF vs. angle for the cylinder shown in Fig. 5 (TM_z mode, $f = 300$ MHz). [Color figure can be viewed in the online issue, which is available at wileyonlinelibrary.com]

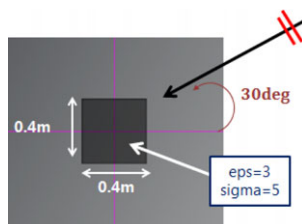


Figure 11 A square-shaped lossy, dielectric cylinder. [Color figure can be viewed in the online issue, which is available at wileyonlinelibrary.com]

C. The 2D Near Field to Far Field Transformation

Because of the finite nature of the FDTD computation space it is impossible to calculate far field response directly; NTFF transformation is essential. So far, many NTFF transformations are proposed but the most commonly used ones are time and frequency domain transformations [7–10]. They both utilize the surface equivalence theorem but their implementations are different so that time domain transformations are more suitable for the case when broadband mono-static response is desired. Likewise, frequency domain transformations are more suitable for the case when bistatic response is sought. Here, frequency domain NTFF transformation is used [11].

IV. RCS2D VIRTUAL TOOL AND EXAMPLES

The front page of the java-based RCS2D Virtual Tool is pictured in Figure 6. It has two distinct EM solvers; MoM and FDTD. The virtual tool can be run with both models and results may be compared in terms of accuracy and computation time.

Highly effective charts and visualization capabilities are included, therefore simulations become attractive. The front page is split into four subpanels. The top panel contains numerous image buttons to improve accessibility. The left panel is divided into two collapsible Workspace and Summary subpanels. Workspace demonstrates all features that are supplied by the program. Summary part provides users to

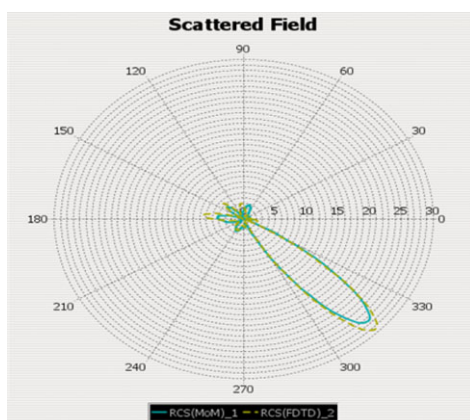


Figure 12 The RCS of dielectric, square object (TE_z mode, $f = 600$ MHz, illumination angle = 30°). [Color figure can be viewed in the online issue, which is available at wileyonlinelibrary.com]

observe all actions as well as computer resources. The right panel has three tabs called Simulation Area, Visualization and Simulation Results. User can draw the geometry via the Simulation Area tab. Visualization tab is reserved for real-time wave monitoring for FDTD based simulations. Simulation Results tab is used as a container for polar charts.

The program provides basic geometries (square, ellipse and polygon) to make drawings easy. The user can scale, translate, rotate and mirror the objects to the shape from the corresponding tree node located left of the user interface. Another feature is the Drag operation. If objects are overlapped after dragging, new dialog box will pop-up to offer options of object combinations.

To illustrate the power of RCS2D several tests with various materials and geometries are performed and comparisons are given. MoM and FDTD models are also validated through these tests. First, a C-shaped object is considered (Fig. 7).

Here, a perfectly electrical conductor (PEC) object is taken into account. The size of the object is 1 m (half wavelength at 600 MHz). The object is illuminated from 210° and observation points are located on a circle enclosing the object with 4 m radius. SFs are simulated with both methods and results for the TM_z polarization are shown in Figure 8. As observed, perfect agreement is obtained.

Next, the infinite cylinder with the cross section shown in Figure 9 is taken into account. The cylinder is formed of two lossy dielectric parts. This cylinder is illuminated by a PW from top (with the angle of 90°) and bi-static SFs are recorded all around. The observation points are located at 5 m away. Results for the same polarization are given in Figure 10.

The final example belongs to a lossy dielectric square investigated under the TE_z polarization (Fig. 11). The size of the square is 0.4 m. Observation points are located on a circle enclosing the object with 4 m radius. The object is illuminated by a PW from an angle of 30° . The results are shown in Figure 12.

Note that, SFs around the objects are directly obtained at the specified frequency in MoM. Conversely, broadband PW response is obtained around the object in the near field first with the FDTD model. Far-fields are extrapolated via the FFT plus NTFF transformation.

V. CONCLUSION

A novel RCS2D EM scattering virtual tool is developed. A frequency-domain numerical model, the MoM and a time-domain model, the FDTD are used as core models. Both TM and TE polarized scattering fields may be simulated in RCS2D. EM scattering of arbitrary geometries and different materials under PW illumination can be investigated. This virtual tool can be used in graduate-level EM courses to understand EM scattering phenomena and to gain physical insight.

REFERENCES

1. R.F. Harrington, *Field Computation by Moment Method*, First ed., IEEE Press, New York, 1968; reprinted 1993 by IEEE.

2. J.H. Richmond, TE-wave scattering by a dielectric cylinder of arbitrary cross-section shape, *IEEE Trans Antennas Propag* 14 (1966), 460–464.
 3. R.G. ROJAS, TE-wave scattering by a dielectric cylinder of arbitrary cross-section shape, *IEEE Trans Antennas Propag* 36 (1988), 238–246.
 4. K.S. Yee, Numerical solution of initial boundary value problems involving Maxwell's equations in isotropic media, *IEEE Trans Antennas Propag* 14 (1966), 302–307.
 5. J.P. Berenger, Three dimensional perfectly matched layer for the absorption of electromagnetic waves, *J Comput Phys* 127 (1996), 363–379.
 6. C.J. Railton and J.B. Scheider, An analytical and numerical analysis of several locally conformal FDTD schemes, *IEEE Trans MTT* 47 (1999), 56–66.
 7. A. Taflov and S.C. Hagless, *Computational electrodynamics the finite-difference time domain method*, 2nd edition, Artech House, Boston, 2000.
 8. O.M. Ramahi, Near- and far-field calculations in FDTD simulations using Kirchhoff surface integral representation, *IEEE Trans Antennas Propag* 45 (1997), 753–759.
 9. R.J. Luebbers and K.S. Kunz, M. Schneider, and F. Hunsberger, A finite difference time-domain near zone to far zone transformation, *IEEE Trans Antennas Propag.* 39 (1991), 429–433.
 10. L. Sevgi, *Complex Electromagnetic Problems and Numerical Simulation Approaches*, IEEE Press/Wiley, Piscataway, NJ, 2003.
 11. S.A. Schelkunoff, Some equivalence theorems of electromagnetics and their application to radiation problems, *Bell System Tech J* 15 (1936), 92–112.
-